Journal of Alloys and Compounds 502 (2010) 250–256

Contents lists available at ScienceDirect

Journal of Alloys and Compounds

journal homepage: www.elsevier.com/locate/jallcom

Mechanochemical synthesis of nanostructured SiO_2–SiC composite through high-energy milling

Siti Aishah Kamarul Zaman, Samayamutthirian Palaniandy*, Zuhailawati Hussain

School of Materials and Mineral Resources Engineering, Engineering Campus, Universiti Sains Malaysia, 14300 Nibong Tebal, Penang, Malaysia

ARTICLE INFO

Article history:
Received 14 December 2009
Received in revised form 21 April 2010
Accepted 23 April 2010
Available online 4 May 2010

Keywords:
Silicon carbide
Nanocomposite
Milling

ABSTRACT

Under ambient conditions, silica (SiO_2) and graphite (C) were milled in a ring mill at up to 18 000 s, followed by heat treatment at 1000 °C. A SiO_2–SiC nanocomposite with a ratio of 86.3:13.7 was obtained. The formation of an amorphous phase in the powder, the low degree of long-range order in the remaining crystalline particles, the large grain boundaries associated with the ultrafine crystallites, the high internal strain in the remaining crystalline SiO_2, the ultrafine particle size, and the intimate mixing of reactants increased the reaction kinetics and reaction driving force for the SiC phase in the nanocomposite.

1. Introduction

Metal carbides exhibit great hardness, high melting points, and chemical stability at room temperature, which make them important materials for engineering applications. Among the carbides, silicon carbide (SiC) is widely used in abrasives, cutting tools, bullet-proof vests, high-performance ceramic disc brakes, filler materials, and as catalyst support [1,2]. SiC is an excellent filler material as it exhibits high fracture strength, excellent creep and wear resistance, good thermal conductivity, low coefficient of thermal expansion, and high thermal and chemical stability under severe service conditions. SiC is produced through various methods and the traditional production method is done through powder metallurgy route by heating the mixture of SiO_2 and C at 2000–2300 °C for 30 h. This is called the Acheson process [3]. The SiC particles from the Acheson process exhibit large crystallite sizes and suffer the contamination of oxygen. In addition to this process, SiC is also produced by polymer pyrolysis, chemical vapour deposition, hot pressing, and liquid phase reaction. These processes require temperatures higher than 1500 °C for the formation of SiC phases [1]. The higher cost of high-temperature processing increases the production cost of end products, which is considered a major disadvantage in developing countries. However, SiC can be synthesized through a mechanochemical method at room temperature in high-energy mills such as SPEX, planetary ball, and stirred mills. During the mechanochemical synthesis, pure Si powder is mixed with graphite at 1:1 ratio and the mixture is milled longer (i.e., 40 h) for the formation of SiC. The advantages of mechanochemical synthesis include low processing cost, energy efficieny, and high-purity products. However, it also exhibits disadvantages such as the contamination of both the milling media and the mill atmosphere [1].

Among the metal oxides, silica exhibits several excellent properties that are useful in engineering application, especially as a filler material, including good abrasion resistance, electrical insulation, high thermal stability, and, with the exception of hydrogen fluoride (HF), insolubility in all acids. Silica is widely used in ceramics, refractory materials, glass, foundry sand, building materials, investment casting, and as fillers for polymers. The similarity of silica to SiC, in terms of thermal and chemical stability, makes it a good candidate for filler application in various engineering products such as polymer composites [4]. Alternatively, the application of composite filler SiC/SiO_2 is believed to enhance the properties of composites such as polymers. Moreover, silica is cheaper and more easily obtained compared to SiC, which reduces the production cost of end products. This paper focuses on the mechanochemical synthesis of SiO_2–SiC composites through high-energy milling in an oscillating mill, followed by heat treatment of the milled products at a lower temperature, in order to enhance the formation SiO_2–SiC composite phases.

2. Experimental

High-purity silica (99% SiO_2) and graphite (99% C) were used as starting materials in this work. Silica and graphite were mixed at 1:1 atomic ratio. Milling was carried out under varied milling times in a ring mill, which consisted of three steel rings as grinding media. Table 1 shows the chemical composition of silica and graphite. The mill works through friction and impact caused by the movement of the rings and the concentric cylinder, which are placed within a casing that contains the materials

* Corresponding author. Tel.: +60 45996132; fax: +60 45941011.
E-mail address: samaya@eng.usm.my (S. Palaniandy).

0925-8388/$ – see front matter © 2010 Elsevier B.V. All rights reserved.
doi:10.1016/j.jallcom.2010.04.158

Table 1
Chemical composition of silica and graphite.

Composition		Al_2O_3	C	SiO_2	K_2O	CaO	Fe_2O_3	NiO	CuO	ZrO_2
Weight (%)	Silica	0.2	–	99.0	0.026	0.015	0.054	0.016	Trace	Trace
	Graphite	–	99.0	–	–	–	–	–	–	–

Table 2
Milling conditions.

Parameter	Value
Milling media weight (kg)	5.92
Media filling (%)	42.7
Media to powder ratio (%)	12.8
Amplitude (mm)	8
Media density (kg/m^3)	7450
Mill diameter (cm)	22
Mill height (cm)	4.8
Milling media diameter (cm)	18.5, 13.5 and 8.0

to be ground. Mechanochemical synthesis was carried out under atmospheric conditions and the total amount of materials was 100 g for each milling procedure. The milling periods chosen in this work were 30 s, 60 s, 300 s, 600 s, 900 s, 1200 s, 1800 s, 3600 s, 7200 s, and 18 000 s. The milling conditions are summarized in Table 2. X-ray fluorescence was used to determine the chemical composition of the raw materials. The particle size distribution of the samples was measured by laser diffraction method in SYMPATEC, dry mode. The parameter used in the particle size distribution data were volume moment diameter, $d(4.3)$, and span value. Diameter $d(4.3)$ was preferred to the mean particle size because the milled particles exhibited polymodal distribution. Diameter $d(4.3)$ was calculated by SYMPATEC with x_k number percentage of detected diameter d_k, as shown in Eq. (1) [5]. The span value, ψ, which quantifies the particle size distribution, was calculated using Eq. (2), with the values obtained from the particle size analysis data [6]. The diameter was i% smaller than d_i (i = 10%, 50%, and 90%).

$$d(4.3) = \frac{\sum x_k d_k^4}{\sum x_k d_k^3} \tag{1}$$

$$\varphi = \frac{d_{90} - d_{10}}{2d_{50}} \tag{2}$$

The X-ray diffraction (XRD) patterns were collected using a Bruker D8 powder diffractometer, and Kα of Cu (λ = 1.542 A) was used for all the analysis at 40 kV and 20 mA. The XRD pattern was recorded in the range 2θ = 15–70° using a step size of 0.050 and a counting time of 5 s per step. Silicon powder was used as a standard to remove the instrumental broadening effects from the observed profile broadening. Line positions, intensities widths and shapes were obtained from the XRD spectra in order to characterize the microstructure in terms of defects parameter such as crystalline size and microstrain. The APD version 4.1 g software was used to obtain these parameters. The $K_{\alpha 2}$ component was removed from the XRD spectra with the assumption that $K_{\alpha 2}$ intensity was half of the $K_{\alpha 1}$ intensity. The (1 0 1) plane was selected for the profile analysis. The overlapped peak was split using the APD version 4.1 g software. The X-ray diffraction patterns were adjusted to a combination of Cauchy and Gaussian line shape, using the Halder and Wagner method for obtaining the physical broadening as shown in Eq. (3) where β_f, β_h and β_g are the integral breadths of the instrumental, observed and measured profiles respectively. The profile fitting procedure was performed without smoothing the XRD spectra. Each goodness factor was refined to a value of <5% for all the reflections. Maximum height of the peak (I_{max}), integral breath of line profile ($\beta = A/I_{max}$), full-width at half maximum (FWHM) and peak position (2θ) were obtained from the adjusted line profile. A is the area under the peak. The apparent crystallite size was calculated using the Scherrer Equation as shown in Eq. (4). The Scherrer formula describes the mutual dependence between the line profile integral breath and crystallite size, D_v which was the volume weighted mean of the crystallite in the direction perpendicular to the diffracting planes; the constant varied with the reflection Bragg angle and crystallite shape. Lattice strain was calculated using Eq. (5). The structural disorder due to increasing abundance of X-ray amorphous material was manifested through the reduction in the integral intensity of diffraction lines [4]. The relative fractional amorphization (Am) defined in Eq. (6) was based on the area under the (0 0 2) peak where A_0 and and A is the area under the peak for feed and ground sample respectively [4].

$$\beta_f = \frac{\beta_h^2 - \beta_g^2}{\beta_h} \tag{3}$$

where β_f, β_h and β_g are the integral breadths of the instrumental, observed and measured profiles respectively [4].

$$D_v = \frac{K\lambda}{\mathrm{FWHM}}\cos\theta \tag{4}$$

where D_v is volume weighted mean of the crystallite size, K is the constant, θ is the Bragg angle of ($h\,k\,l$) reflection and λ is the wavelength of X-rays used [4].

$$\varepsilon = \frac{\beta}{4\tan\theta} \tag{5}$$

where ε is lattice strain [4].

$$\mathrm{Am} = \frac{A_0 - A_t}{A_0} \times 100 \tag{6}$$

where Am is fractional amorphization. A_0 and and A_t are the area under the peak for feed and ground sample respectively [4].

The morphology of the sample was observed by scanning electron microscopy (JOEL, ZEISS, Supra). The carbothermic reduction was conducted in a tube furnace under ambient conditions. The average heating rate was 10 °C/min and the sample was held at 1000 °C for 1 h.

3. Results and discussion

3.1. Mechanochemical synthesis

In order to determine the phase changes during the mechanochemical synthesis, the milled product was picked up for XRD analysis. Fig. 1(a) shows the XRD of the milled powder at various milling times. The sample, which was milled for 5 h, underwent heat treatment at 1000 °C in a furnace under atmospheric conditions. Fig. 1 shows that as the milling progressed, the silica and carbon phases underwent mechanochemical effects, exhibiting reduction in peak intensity, peak base broadening and peak shift to lower angle. The reduction in the peak intensity in the early stage of milling is drastic, whereas a rapid decrease was observed for silica phase (1 0 1) within 1 h, and came to a plateau 1 h after that. The gradual reduction of the peak intensity of silica and carbon was observed as the milling progressed. The (1 1 0), (1 0 2), (3 0 1), (1 1 1), (2 0 0), (2 0 1), and (2 0 2) plane reflection peaks of silica vanished after 3600 s of milling. The (0 0 2) plane of graphite overlapped with the (1 0 1) plane of silica.

In order to observe the amorphization of graphite, the (1 0 0) plane at 42.2° was taken into consideration, which became fully amorphous after 1800 s. Ghosh and Pradhan mentioned that the absence of graphite reflection patterns in the XRD pattern may be attributed to the following reasons: (i) the carbon atoms occupy interstitial positions in the Si lattice, (ii) thin graphite particles stick into the intergrain boundaries of Si grains, or (iii) the amorphization of graphite layers [2]. The preserved reflection of the remaining crystalline SiO_2 exhibited broadening, which suggests smaller crystallite sizes and the presence of internal strain. Initial SiC formation started at 30 s, when a minor peak of γ-SiC was observed at 2θ = 44.5° and the intensity of this peak increasing as the milling progress till 5 h. Fig. 1(b) shows the heat treated sample that was ground for 18 000 s and it exhibits the occurrence of five phases where α-SiC, β-SiC, quartz, and cristobalite phases occurs due to mechanochemical process of SiO_2 and C whilst iron chromium oxide phase was detected due to the contamination from the grinding media for longer milling time. The iron chromium oxide phase was not detected in the milled samples prior to heat treatment may cause by stress induce by the milling media on the iron chromium oxide particles. After heat treatments, the stress in the particles is relief which lead to the increase in the peak intensity. Mild acid leaching is one of the methods that can be adopted in order to remove the iron chromium oxide from the nanostructured SiO_2–SiC composite and its needs further detail study.

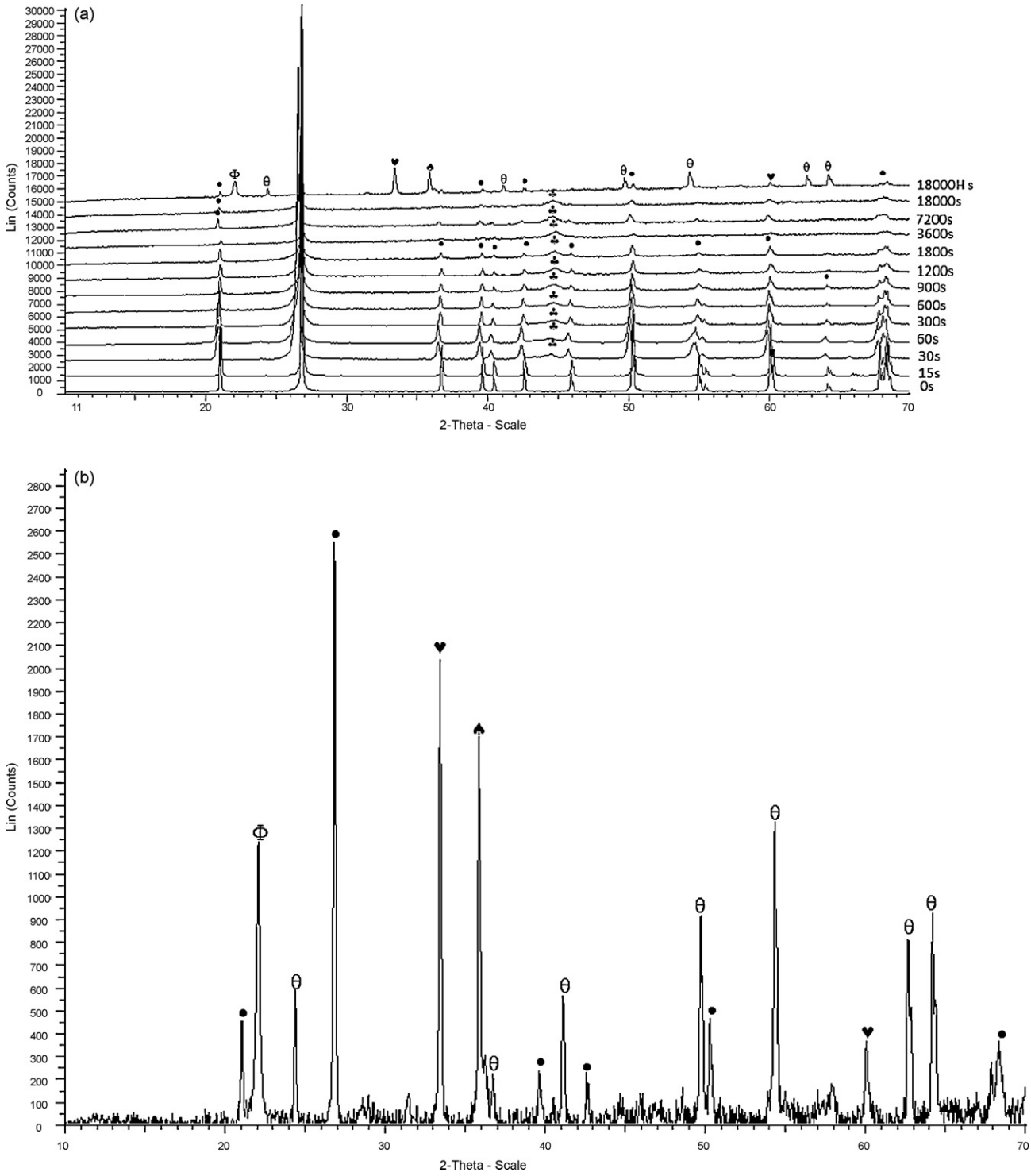

Fig. 1. X-ray diffraction of unmilled, milled, and heat treated powders (●, SiO_2; ♥, α-SiC; ♠, β-SiC; ♣, γ-SiC ♦, C; Φ, crystobalite and θ, iron chromium oxide).

Fig. 2 shows the reduction of the degree of crystallinity of SiO_2 and C, and the degree of formation of the SiC (1 0 0) reflection plane as milling progressed. Twelve point nine percent (12.9%) of SiC was formed after 18 000 s of milling. The formation of the SiC phase started at 3600 s, as shown in Fig. 2, and it progressively increased as the milling time increased. Based on this observation, prolonged milling for more than 18 000 s will further amorphize the SiO_2 phase and increase the formation of the SiC phases. The degree of formation was calculated using Eq. (7), where I_{SiO_2}, I_C, and I_{SiC} are the intensities of SiO_2, C, and SiC phases, respectively. The heat treatment for 1 h at 1000 °C formed 13.7% of the SiC phase and resulted in a composite consisting of 86.3% SiO_2 and 13.7% SiC in nanostructured form.

Many studies have carried out work on the preparation of nanostructured SiC through the high-energy milling of elemental Si and C as starting materials because the reaction between elemental Si and C has negative free energy of formation, as shown in Eq. (8). Meanwhilst, the process using SiO_2 and C as starting materials has large positive free energy of formation at room temperature with 1 atm of CO_2, as shown in Eq. (9) [1,2]. Ren et al. [3] have produced SiC

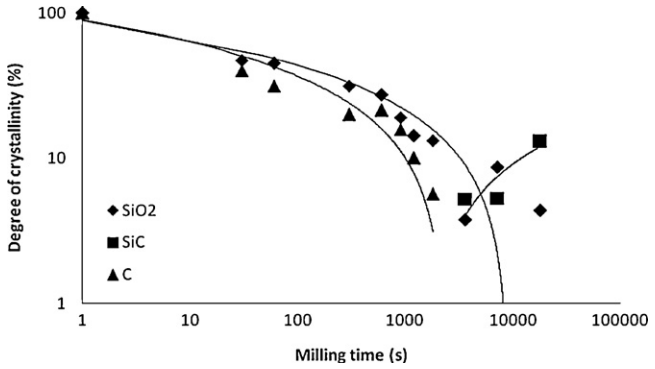

Fig. 2. Peak intensity of SiO_2, C and SiC as a function of milling time.

through an integrated mechanical and thermal activation process where SiO_2 and C were milled in an attritor mill and was followed by heat treatment at 1400–1500 °C. The milling was carried out up to 48 h and the mill speed was maintained at 600 rpm. The XRD results showed the absence of a SiC phase in the milled samples. In this study, SiC formation was observed at the early stage of milling. This phenomenon is very much related to the amount of energy delivered by the mill to the particles. In the Ren et al. study [3], the amount of SiC formation was almost 100% after 48 h of milling, with the milling and heat treatment performed under inert conditions. In this work, both the milling and the heat treatment were carried out in ambient air, causing carbon to react with oxygen in the air to form CO_2, which may have led to an insufficient amount of C reacting with SiO_2, resulting in the SiO_2–SiC powder composite. This present study of high-energy milling in a ring mill has resulted to changes in the formation of an amorphous phase in the SiO_2 and C powder mixture, the low degrees of long-range order in the remaining crystalline particles, and the large grains with ultrafine crystallites with high internal strain.

Mechanical milling is an alternative method to produce powder in new phases. SiO_2 and C are subjected to high-energy collision in oscillating mills, causing the powder to be fractured and cold-welded. Fracturing and cold welding enables these powders to be in contact with each other and atomically clean surfaces with minimized diffusion distance; hence, producing laminated structures. These laminated structures are further refined as the fracture takes place and as their thickness decreases. At this stage, dissolution may occur but the chemical composition is not homogeneous. A composite of SiO_2–SiC phases results. The relationship between the milling time and the degree of crystallinity for SiO_2 and C, and the degree of formation of SiC is shown in Eqs. (11)–(13), respectively. This indicates that the amorphization rate of graphite is higher as compared to SiO_2, due to the differences in terms of hardness. In addition, Eq. (12) indicates that a further increase in the milling time will form more SiC phases. These models can be used as an indicator to optimize the mechanochemical reaction process.

$$\text{degree of formation} = \frac{I_{SiC}}{I_{SiO_2} + I_C + I_{SiC}} \quad (7)$$

$$Si + C = SiC \quad \Delta G_{298} = -70\,850\,\text{J/mol} \quad (8)$$

$$SiO_2 + 2C = SiC + CO_2 \quad \Delta G_{298} = 389\,320\,\text{J/mol} \quad (9)$$

$$DOC = -9.742\ln(t) + 88.608 \quad (10)$$

$$DOC = -11.56\ln(t) + 89.76 \quad (11)$$

$$DOC = 4.929\ln(t) - 36.319 \quad (12)$$

The mixing mechanism of the SiO_2–C mixture is an important criterion as it will influence carbothermic reaction. It is essential to know whether SiO_2 and C are intimately mixed at atomic levels (i.e., the formation of chemical bonds between Si and C, or the van der Waals bonds between SiO_2 and C), or just physically mixed at microstructural level after prolonged milling, as the amount of mixing will affect the formation mechanism of SiC during the heat treatment. Undoubtedly, prolonged high-energy milling leads to a more uniform mixing of SiO_2 and C at a microstructure level due to repetitive plastic deformation, fragmentation, and cold welding during the milling. Ren et al. [3] reported that SiO_2 and C physically separate in the early stages of milling, and that prolonged milling causes some of the SiO_2 and C to mix intimately; however, there was no evidence of SiO_2 and C mixed at atomic levels. In this work, the formation of SiC phases, indicated by X-ray diffraction patterns during the milling itself, prove that Si and C mix at atomic levels.

The main issue regarding the foregoing phenomenon is the amount of energy delivered by the mill and the milling mechanism. The energy delivered by the attritor mill ranged between 200 kW/ton and 400 kW/ton, whilst a ring mill delivers 1690 kW/ton of energy, based on the calculation of its kinetic energy. The huge differences in delivered energy permit the formation of SiC during the milling itself, as compared to the attritor mill. Mixing at atomic levels requires that the powder constituents have shearing capabilities so that shearing of atomic planes can take place during plastic deformation. It has been shown that the level of mixing insoluble constituents during milling is closely related to the enthalpy change of the possible chemical reaction in the system under consideration. For SiO_2 and C systems in the Ren et al. study [3], the mixing of SiO_2 and C at atomic levels increased the free energy of the system. If the C is forced into SiO_2 by shearing during plastic deformation and if the carbon can diffuse fast enough at the milling temperature, the carbon will have the tendency to diffuse out of SiO_2. SiO_2 and C thus remain atomically separated. In this work, Si and C are atomically bonded, which indicates that carbon did not diffuse out from SiO_2. This phenomenon may be related to the construction of ring mills with high media filling, and a low media-to-powder ratio permits the high probability of particles being trapped between the grinding media. This stands in comparison to an attritor mill. The reaction of SiC formation from carbothermic reduction at high temperatures is rather complex, but it is generally agreed that the overall reaction is as shown in Eq. (13). Ren et al. [3] suggested a series of reactions prior to the SiC phase; but, in this work, nucleation of the SiC phase has been obtained during the milling and it was used as a seed for the formation of SiC phases during the heat treatment.

$$SiO_2(s) + 3C(s) = SiC(s) + 2CO(g) \quad (13)$$

The enhanced carbothermic reaction was observed in this study due to finer particle sizes, large surface areas, the intimate mixing of SiO_2 and C at microstructure level, and the formation of SiC seeds during the milling. On the other hand, the formation of an amorphous phase in the powder, the low degree of long-range order in the remaining crystalline particles, the large grain boundaries associated with ultrafine crystallites, the high internal strain in the remaining crystalline SiO_2, the ultrafine particle size, and the intimate mixing of reactants increase the free energy of reactants, thereby increasing the driving force of carbothermic reaction. Finally, iron contamination from the milling media was detected on the sample that was milled for 18 000 s and underwent heat treatment where iron chromium phase was detected at $2\theta = 24.30^\circ$.

Some features of the activation process, particularly the microstructure of the particles, were analyzed through XRD patterns; the crystallite size and lattice strain were evaluated using Eqs. (4) and (5). Figs. 3 and 4 show the crystallite size and lattice strain of SiO_2 and C, respectively. It can be seen that the crystallite size decreased and the internal strain increased rapidly as the

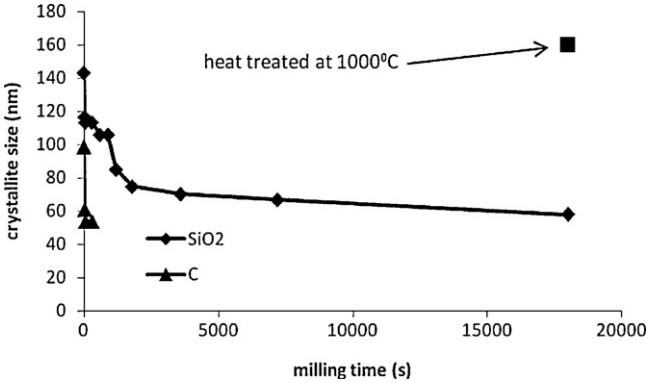

Fig. 3. Crystallite size of SiO_2 and C as a function of milling time.

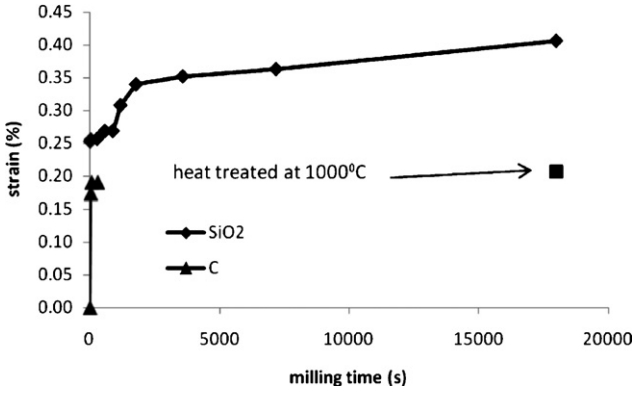

Fig. 4. Lattice strain of SiO_2 and C as a function of milling time.

milling progressed, especially at the early stage, nearing a plateau after 3600 s of milling.

Chaira et al. [1] mentioned that prolonged milling causes the crystallite size to reduce; however, the internal strain is reduced after 20 h of milling due to the formation of a SiC phase. In this test work, the internal strain kept increasing, although there was a formation of a SiC phase, because the SiO_2 phase was not completely changed. The crystallite size and the lattice strain of the graphite were measured until 600 s. The reflection peak at 59.95° diminished after 600 s of milling. The graphite exhibited a rapid diminution of crystallite size compared to silica due to the difference in the material hardness between these two materials.

The crystallite size and lattice strain of SiO_2 increased and decreased, respectively, after heat treatment at 1000 °C for 1 h. This phenomenon was caused by the relaxation of the internal strain after the heat treatment. The average crystallite size of SiO_2–SiC mixture reached 57.9 nm after 18 000 s of milling, which indicates that prolonged milling in oscillating mills produces nanostructured composite particles. The SiC unit cell parameters in cubic form are $a = 3.07$ A and $c = 37.6$ A. During milling, the energy delivered by the mill led to flattened particle surfaces. Flattening was also accompanied by an increase in the dislocation density [7]. Crystallite sizes were used to calculate the dislocation density. To a first approximation, dislocation density was assumed to be at least one dislocation per crystallite. Hence, dislocation density (N) becomes the inverse square of the crystallite size (D_v), as shown in Eq. (14). Fig. 5 shows the dislocation density of SiO_2 and C. The dislocation density increased drastically in the initial stage of milling and then it gradually increased after 1800 s of milling. At smaller crystallite sizes, the generation of dislocation is more difficult compared to a larger crystallite size. As the milling progressed, the crystallite

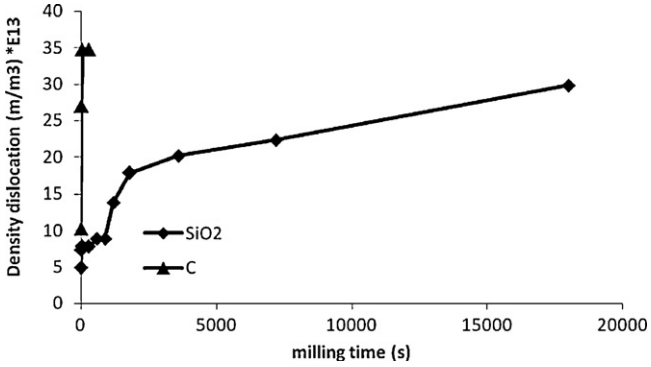

Fig. 5. Dislocation density of SiO_2 and C as a function of milling time.

size reduced, which resulted in difficulties in the dislocation. This phenomenon was observed during prolonged milling, as shown in Fig. 5, for SiO_2. Graphite exhibited a higher value of dislocation density, as compared to SiO_2, because it is softer.

$$N = \frac{1}{D_v^2} \tag{14}$$

3.2. The influence of mechanical activation time on particle size and particle size distribution

The powder particles of SiO_2 and C mixed together in the early stage of milling and were mechanically activated, such that the individual particles of SiO_2 and C formed composite particles. After 3600 s of milling, some amount of SiC was formed in various phases. Fig. 6 shows the volume moment diameter of SiO_2 + C mixture as a function of milling time. At the initial stage of milling up to 600 s, the particle size decreased. It began to increase after 900 s up to 3600s of milling. The increase in particle size indicates that cold welding took place between the SiO_2 and C particles. In TiC system, El-Eskandarany et al. [8] analyzed polished and etched particles at the early stage of milling and showed that individual particles many thick layers of individual layers of the diffusion couples of the constituents powders. They believed that a solid state reaction occured at the clean interface of these layers and that a new single phase was formed after further milling. When the new phase formed, the reactant layers disappeared. Therefore, in such a system, the only means that the particle could grow is by cold welding. A similar mechanism was observed through the increase in particle size after 600 s of milling, which indicates that cold welding between SiO_2 and C took place. The XRD pattern confirmed that the SiC phases began to occur at this milling time. The particle size continued to increasing as the milling progressed up to 1800 s,

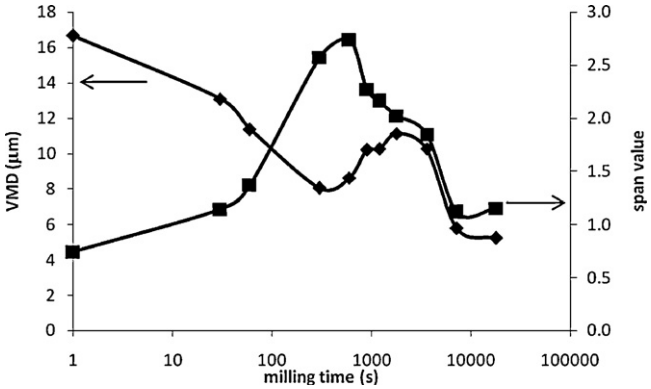

Fig. 6. Volume moment diameter and span value of SiO_2–C mixture as a function of milling time.

and reduced again after 1800 s. This phenomenon indicates that cold welding takes place up to 1800 s of milling, and that further milling reduces the particle size of the newly formed composite phases.

Another interesting phenomenon that should be noted when milling composite materials, especially in the presence of graphite, is the evolution of the particle size of the mixture and of the individual particles. Ren et al. [3] reported the particle size of the milled composites in specific surface areas and mentioned that the increase in specific surface area at the initial stage of milling is dictated by graphite. This indicates that specific surface area is not a good indicator for particle size reduction. The main problem is the delamination of the basal plane of graphite that leads to a higher specific surface area. In this work, the laser particle sizer was used, which gave the actual distribution of the milled particles.

Fig. 7 shows particle size as a function of the milling time of the SiO_2 + C mixture, SiO_2 and C. SiO_2 and C were milled for 30 s, 60 s, 300 s, and 600 s for comparison with the SiO_2 and C mixture. The presence of graphite in the mixture reduces the comminution effect because, at a given milling time, pure SiO_2 exhibits finer particle size compared to SiO_2 + C powder mixture. Furthermore, graphite exhibits a coarser particle size compared to the SiO_2 + C mixture and SiO_2 at a given milling time. This phenomenon indicates that the particle size of the mixture is very much dependent on graphite. The lubricant effect of graphite and the easy displacement of the (0 0 *l*) basal plane cause the decrease in the comminution effect. Further research is needed to reduce the lubricant effect of graphite during milling.

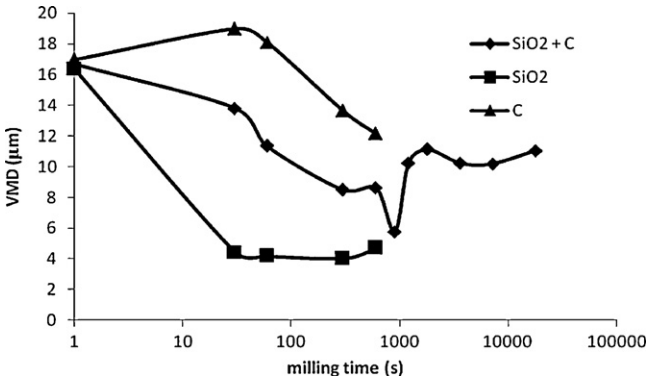

Fig. 7. Volume moment diameter of SiO_2 + C, SiO_2 and C as a function of milling time.

3.3. Particle morphology

Fig. 8 shows photomicrographs of the SiO_2–C mixture as a function of milling time. In the initial stage of milling, the irregular particle shapes of SiO_2 and flaky graphite in the size range of several microns were clearly seen, which indicates the breakage of SiO_2 particles due to the impact and delamination of graphite in the basal plane. At 600 s, as the milling progressed, the particle breakage became even finer, and there was a tendency for these graphite flakes to cover around the silica particles, as shown in Fig. 8(b). At this stage, XRD shows the formation of γ-SiC phase, where it is believed that the reaction between the fresh surface of SiO_2 and C

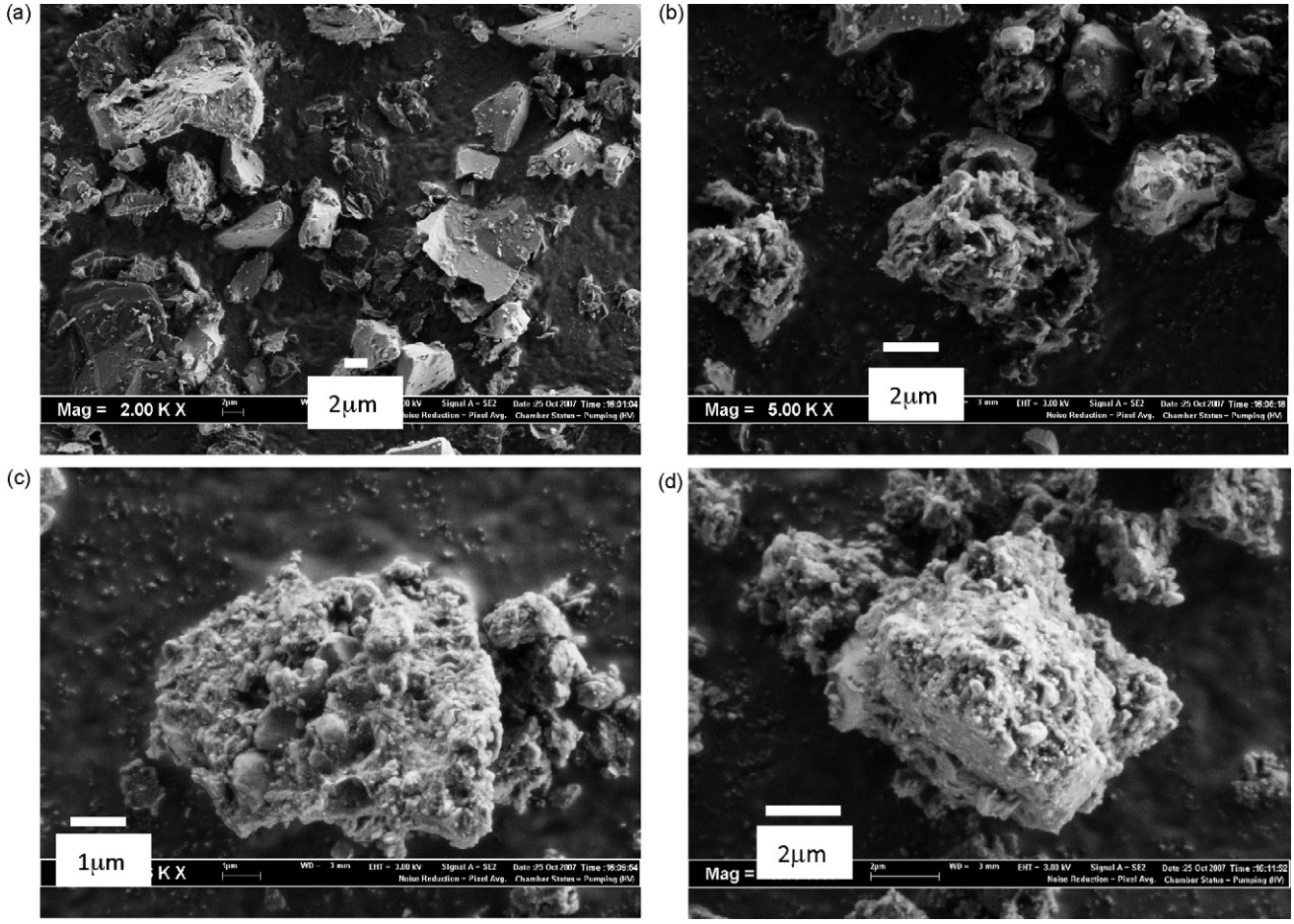

Fig. 8. Photomicrographs of SiO_2 + C mixture as a function of milling time: (a) 30 s, (b) 600 s, (c) 18 000 s, and (d) 18 000 s-heat treated.

takes place due to a continuous impact by the milling media. A massive aggregation of small particles was observed when the mixture was milled for 18 000 s. Smaller particles in the submicron range aggregated to form particle sizes the range of several microns, as shown in Fig. 8(c). The particles that underwent heat treatment still exhibited aggregation, although the XRD microstructure characterization showed internal strain relaxation. The initial particle size of SiO_2 and C was 12.35 μm and 16.99 μm. The aggregate particles exhibited sizes in rounded particles submicron range, and there was no evidence of flaky particles in the micrographs. Ren et al. [3] mentioned that the prolonged milling causes the flakelike structure of graphite powders to agglomerate and become even finer. Hence, they become difficult to discern. This suggests that the graphite flakes are extremely fine and/or the graphite has just become amorphous. This phenomenon shows the formation of SiC phases as the C is used.

Juhasz and Opoczky [9] suggested that there are three stages of interaction between the particles, namely, adherence, aggregation, and agglomeration. In the adherence stage, the particles will coat the mill body and the grinding media. At the aggregation stage, the particles associate weakly by van der Waals-type adhesion, which is a reversible reaction. Agglomeration is defined as a very compact, irreversible interaction of particles with the occurrence of chemical bonding between the particles. In the case of high-energy milling of SiO_2 and C in oscillating mills, the interaction between particles is considered as agglomeration because there is new phase formation resulting from the reaction between these two phases.

4. Conclusion

This study showed that there is a possibility to obtain SiC phase, in a comparatively shorter milling time, through the high-energy milling of SiO_2 and C in a ring mill. In this case, the formation of SiC–SiO_2 nanocomposite phases was obtained as milling and heat treatment were carried out under ambient conditions. The nanocomposite obtained was a mixture of 86.3% SiO_2 and 13.7% SiC. The nanostructured SiO_2–SiC composite exhibits amorphism with high inrenal strain in the particles. Furthermore the phase change of quartz to cristobalite was manifested after the heat treatment and contamination from the milling media was observed as well.

Acknowledgements

The authors wish to gratefully acknowledge Universiti Sains Malaysia for granting the research fund under Research University Grant-Fundamental (project no. 811072) for this project.

References

[1] D. Chaira, B.K. Mishra, S. Sangal, Materials Science and Engineering A 460–461 (2007) 111–120.
[2] B. Ghosh, S.K. Pradhan, Journal of Alloys and Compounds 486 (2009) 480–485.
[3] R. Ren, Z. Yang, L.L. Shaw, Journal of American Ceramic Society 85 (2002) 819–827.
[4] S. Palaniandy, K.A. Mohd Azizli, H. Hussin, S.F. Saiyid Hashim, International Journal of Mineral Processing 82 (2007) 195–202.
[5] Lecoq O. Guigon, P.M.N. Pons, Powder Technology 105 (1999) 21–29.
[6] M. Nakach, J.R. Authelin, A. Chamayou, J. Dodds, International Journal of Mineral Processing 74S (2004) S173–S181.
[7] T. Raghu, R. Sundaresan, P. Ramakrishnan, T.R. RamaMohan, Materials Science and Engineering A 304–306 (2001) 438–441.
[8] M.S. El-Eskandarany, K. Sumiyama, K. Suzuki, Journal of Materials Research 10 (3) (1995) 659–667.
[9] A.Z. Juhasz, Opoczky, Mechanical Activation of Minerals by Grinding: Pulverizing and Morphology of Particles, Ellis Horwood Limited, Chichester, 1990.